PERGAMON

Journal of Structural Geology 24 (2002) 743–762

JOURNAL OF STRUCTURAL GEOLOGY

www.elsevier.com/locate/jstrugeo

# Extensional fault-related folding, northwestern Red Sea, Egypt

S.M. Khalil[1], K.R. McClay*

*Fault Dynamics Research Group, Geology Department, Royal Holloway University of London, Egham, Surrey TW20 0EX, UK*

Received 7 August 2000; accepted 1 June 2001

**Abstract**

The Duwi and Hamadat areas on the northwestern margin of the Red Sea rift system exhibit superb outcrop examples of kilometric scale, extensional fault-related folds. In this area, the Nakheil and Hamadat faults of the Rift border fault system consist of a series of WNW- and NW-trending segments that link through breached relay ramps. The fault hanging walls are characterised by a series of offset synclines with non-linear axial traces sub-parallel to the faults. The synclines are doubly plunging and, in the immediate hanging wall to the normal faults, the strata dip sub-parallel to the fault. These folds result from along-strike displacement variations on the individual fault segments together with extension-related fault-propagation folding as the faults propagated upwards through a highly anisotropic pre-rift sedimentary section. In the Duwi area, the axial traces of the synclines are offset and bend in the regions of relay ramps. In the Hamadat area, the synclines associated with individual fault segments are separated by transverse hanging-wall anticlines that formed where segment linkage occurred. Numerical simulations of extension-related fault-propagation folding using a trishear model produce geometries that closely match those of the Duwi and Hamadat folds. The dimensions of these hanging-wall synclines and their relationships to fault displacement variations indicate that they are formed by extensional fault-propagation folding rather than by frictional drag along the fault surface. 

*Keywords*: Extensional fault-related folding; Breached relay ramps; Synclines

## 1. Introduction

Fault-related folding in extensional basins has been the focus of much recent research. Schlische (1992, 1995) described fold systems associated with extension in the Newark basin, eastern USA; Janecke et al. (1998) described examples of extensional folds from the Rocky Mountain Basin and Range province, USA; Gawthorpe et al. (1997), Gupta et al. (1999), and Sharp et al. (2000) have described extensional fault-propagation folding in the eastern Gulf of Suez, Egypt; Maurin and Niviere (1999) analysed extension-related folding in the Rhine graben; Keller and Lynch (1999) described extension-related folding in Nova Scotia, eastern Canada; and Corfield and Sharp (2000) have documented extensional fault-propagation folding in the Halten Terrace, offshore mid-Norway. In particular these studies have highlighted the complex nature of hanging-wall deformation features that may arise in normal fault systems.

Extensional fault-related folds (cf. Schlische, 1995) include:

1. Hanging-wall fault-bend folds generated by changes in dip of the fault surface (cf. rollover anticlines and ramp synclines in seismic sections and in analogue models (e.g. McClay, 1990)).
2. 'Normal drag' folds caused by frictional resistance along the normal fault plane where hanging wall beds are dragged up the fault surface and footwall beds are dragged down the fault surface (cf. Twiss and Moores, 1992; Davis and Reynolds, 1996; Peacock et al., 2000).
3. 'Reverse drag' folds where the hanging-wall beds bend down towards the fault surface and footwall beds flex upwards (cf. Hamblin, 1965; Barnett et al., 1987). In many cases hanging-wall reverse drag is synonymous with rollover anticlines (cf. Peacock et al., 2000);
4. 'Transverse folds' (Schlische, 1995; Janecke et al., 1998) generated by displacement variations along the strike of the fault. These folds have axes perpendicular or at high angles to the fault surface.
5. 'Fault-propagation folds' produced by folding ahead of a propagating fault tip line (e.g. Allmendinger, 1998; Hardy and McClay, 1999; Corfield and Sharp, 2000; Sharp et al., 2000). In some papers these have been

* Corresponding author. +44-1784-443618; fax: +44-1784-438925.
*E-mail address:* ken@gl.rhul.ac.uk (K.R. McClay).
[1] Now at Department of Geology, Faculty of Science, Suez Canal University, Ismalia, Egypt.

0191-8141/02/$ - see front matter 
PII: S0191-8141(01)00118-3

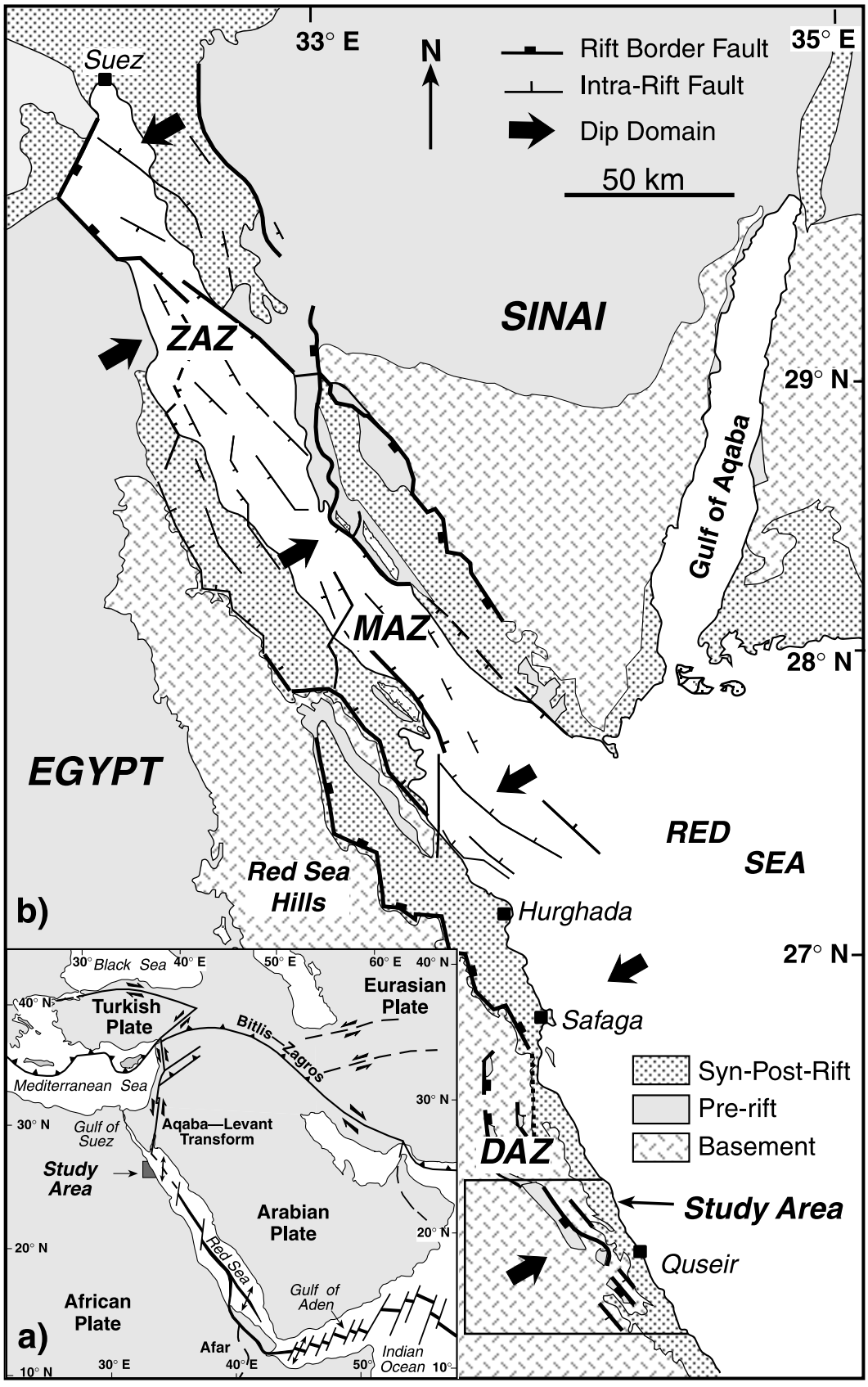
33° E
35° E
N
Rift Border Fault
Intra-Rift Fault
Dip Domain
50 km
Suez
SINAI
ZAZ
29° N
Gulf of Aqaba
MAZ
28° N
EGYPT
RED
SEA
Red Sea
Hills
b)
Hurghada
27° N
Safaga
Syn-Post-Rift
Pre-rift
Basement
DAZ
Study Area
Quseir
30° Black Sea 40° E
50° E
60° E 40° N
Eurasian
Plate
40° N
Turkish
Plate
Bitlis—Zagros
Mediterranean Sea
30° N
30° N
Gulf of
Suez
Aqaba—Levant
Transform
Study
Area
Arabian
Plate
20° N
20° N
Red Sea
Gulf of
Aden
African
Plate
a)
Afar
Indian
Ocean
10° N
30° E
40° E
50°
10°

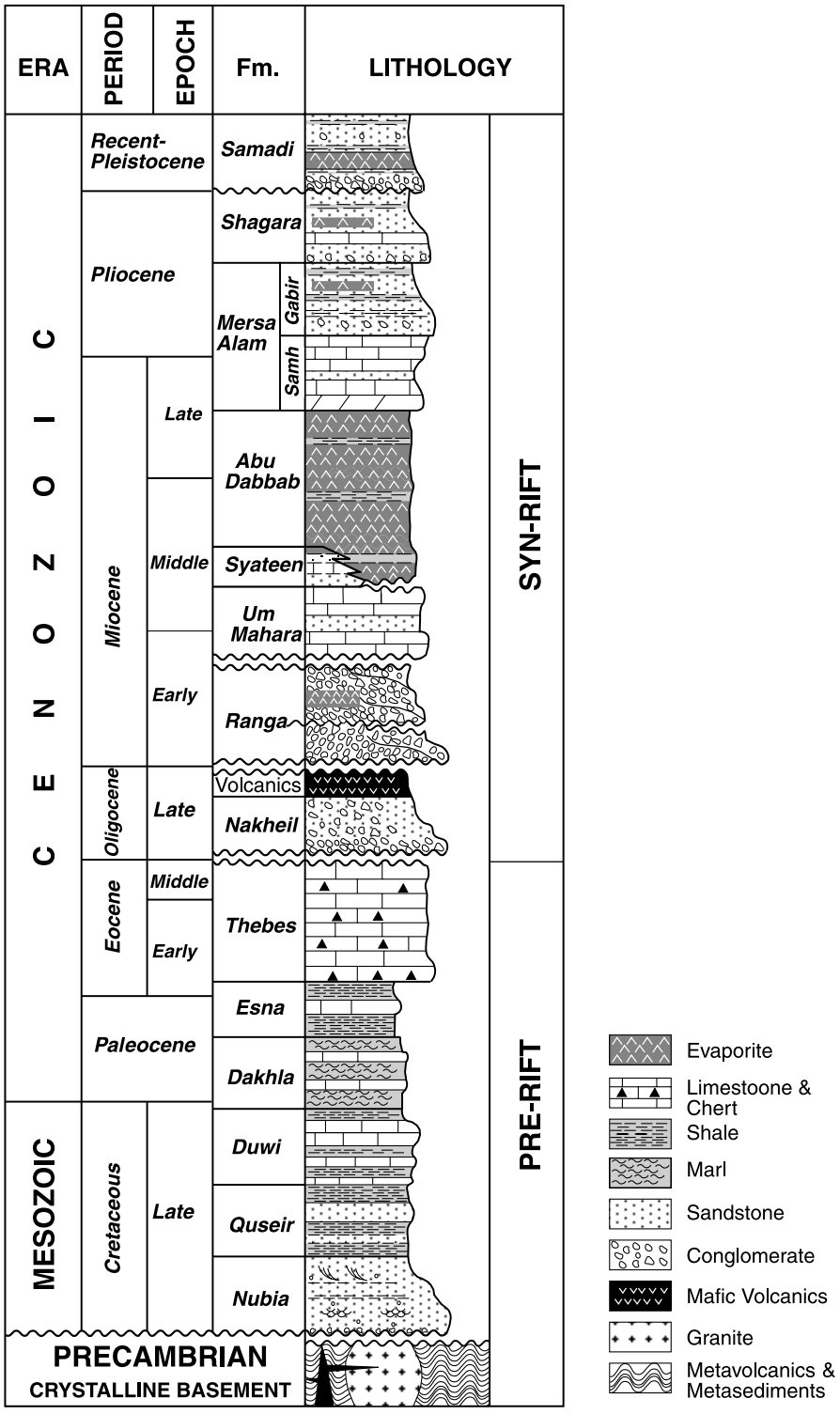


Fig. 2. Summary stratigraphy of the northwestern Red Sea rift system. Data from Said (1990), Purser and Bosence (1998) and the authors' own work.

Fig. 1. (a) Plate tectonic setting of the northwestern Red Sea rift system (modified after Hempton, 1987). (b) Principal structural elements of the northwestern Red Sea–Gulf of Suez rift system. Bold arrows indicate the dominant stratal dip directions within the individual half-graben sub-basins. ZAZ, MAZ and DAZ are the Zaafarana, Morgan and Duwi accommodation zones, respectively.

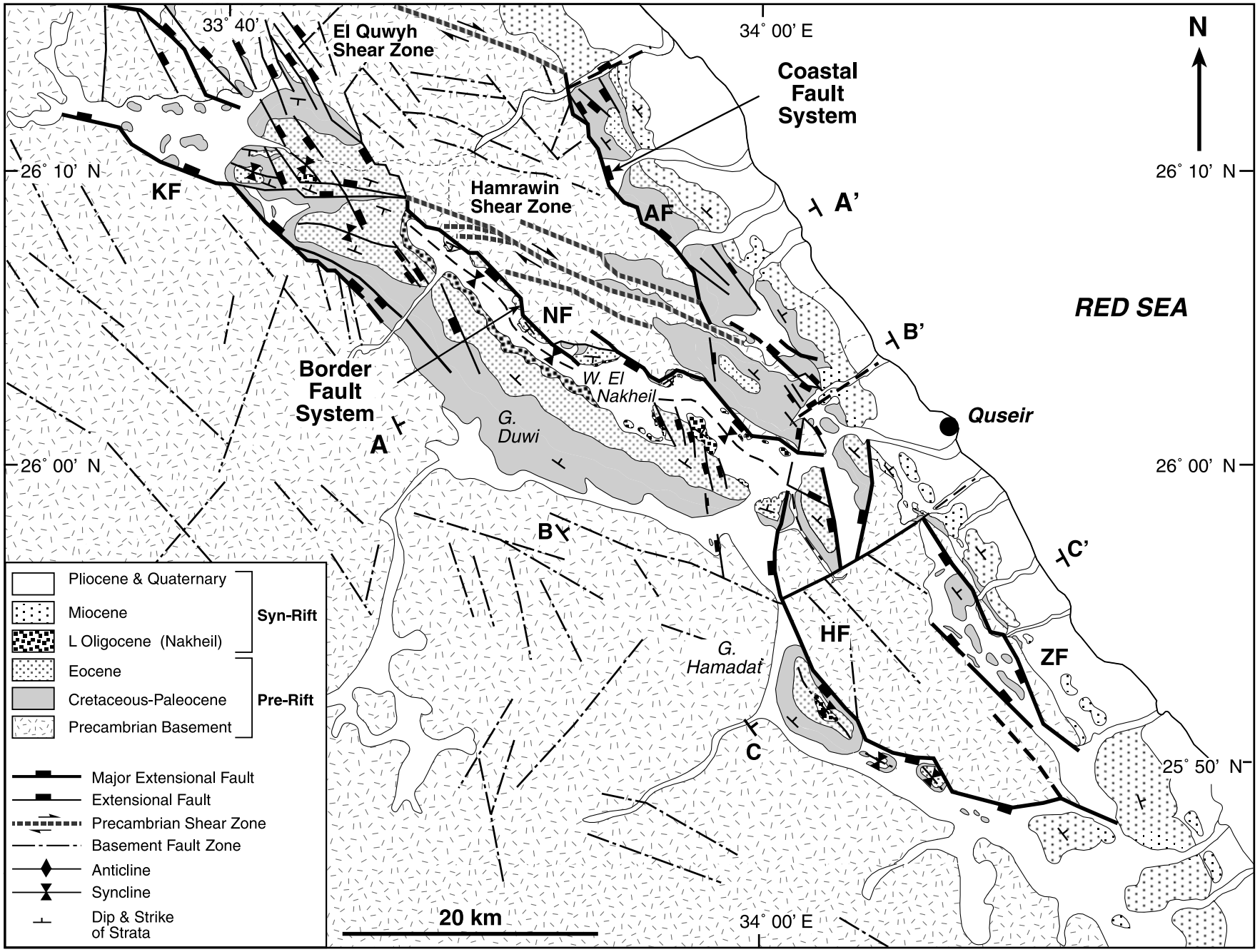
33° 40'
El Quwyh
Shear Zone
34° 00' E
Coastal
Fault
System
N
26° 10' N
KF
Hamrawin
Shear Zone
AF
A'
RED SEA
NF
B'
Border
Fault
System
A
W. El
Nakheil
G.
Duwi
Quseir
26° 00' N
B
C'
HF
ZF
G.
Hamadat
C
25° 50' N
20 km
Pliocene & Quaternary
Miocene
L Oligocene (Nakheil)
Eocene
Cretaceous-Paleocene
Precambrian Basement
Syn-Rift
Pre-Rift
Major Extensional Fault
Extensional Fault
Precambrian Shear Zone
Basement Fault Zone
Anticline
Syncline
Dip & Strike
of Strata

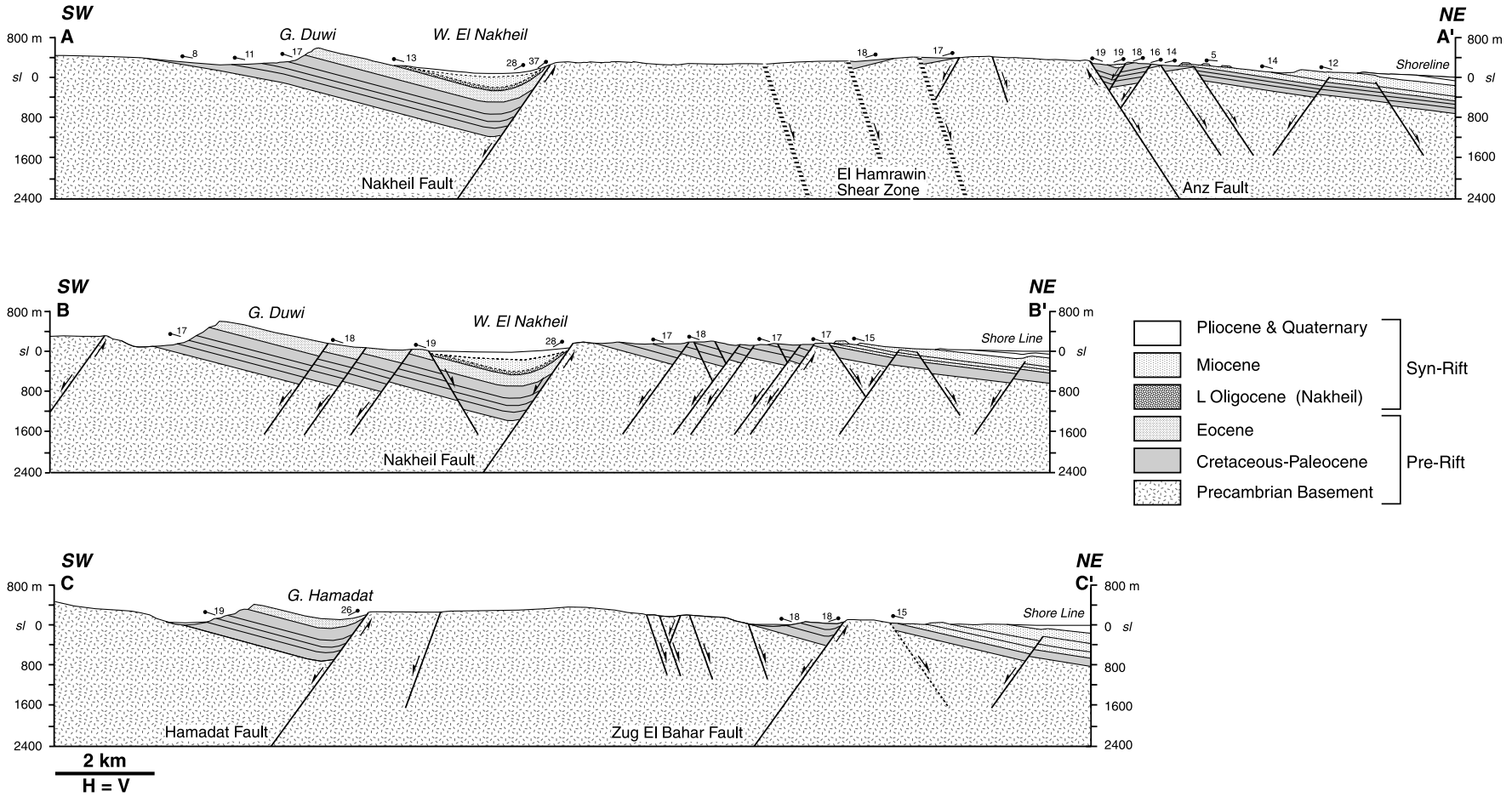


Fig. 3. (a) Simplified geologic map of the Gebel Duwi–Gebel Hamadat area, northwestern Red Sea. KF, NF and HF indicate the Kallahin, Nakheil and Hamadat fault segments of the Border fault system, respectively, and AF and ZF indicate the Anz and Zug El Bahar fault segments of the Coastal fault system. (b) Regional cross-sections across the Gebel Duwi–Gebel Hamadat area (locations are shown in (a)).

termed 'forced folds' (Stearns 1978; see also a comprehensive review by Cosgrove and Ameen, 1999).
6. Compactional 'drape' folds produced by differential compaction of sediments over a pre-exisiting extensional fault scarp.

The aim of this paper is to describe two well-exposed examples of fault-related hanging wall fold systems in the northwestern Red Sea margin, Egypt and to propose models for their 3D development. Analysis of Landsat TM images, aerial photographs combined with detailed geological mapping, and section construction has permitted determination of the 3D fold geometries. Previous interpretations attributed these folds to sinistral strike-slip motion on the bounding faults (Jarrige et al., 1986; Montenat et al., 1988, 1998). Here an alternative model is proposed whereby the folds were produced by both extensional fault-propagation folding as well as by along-strike variations in normal fault displacements. The results of this field study are compared with numerical models of extensional fault-related fold systems.

## 2. Stratigraphic and structural framework of the northwestern Red Sea, Egypt

The Red Sea rift system was formed in the Late Oligocene–Early Miocene in response to the NE separation of Arabia away from Africa (cf. McKenzie et al., 1970; Le Pichon and Francheteau, 1978; Meshref, 1990; Morgan, 1990; Coleman, 1993; Purser and Bosence, 1998). In the Late Middle Miocene, continued opening of the Red Sea became linked to sinistral offset along the Gulf of Aqaba–Levant Transform (Fig. 1a; Freund, 1970; Ben-Menahem et al., 1976; Steckler et al., 1988). The extension direction was N60°E from the Late Oligocene through the Miocene (Bosworth and McClay, 2001). Dixon et al. (1987), Moustafa (1997) Younes et al. (1998), and Younes and McClay (2001) have shown that pre-existing basement fault zones such as NW-trending shear zones of the Najd system in the Arabian plate (Davies, 1984) were reactivated during the Late-Oligocene–Miocene extension. These Precambrian fault zones strongly controlled the orientations of the Cenozoic rift faults.

The northwestern Red Sea–Gulf of Suez rift consists of four distinct sub-basins (with half-graben geometries) separated by complex accommodation zones. In this paper the term 'accommodation zone' refers to a complex zone of faulting that accommodates an along-strike change in both the fault dips and in sub-basin polarity within a rift system (similar usage to that of Bosworth (1985), Rosendahl et al. (1986), and Faulds and Varga (1998)). These accommodation zones are generally oblique to the rift trend (Fig. 1b) (Moustafa, 1976, 1997; Bosworth, 1995; Coffield and Schamel, 1989; Khalil and McClay, 2001). Each sub-basin is asymmetric, bounded on one side by a major NW-trending border fault system whose throw is commonly of the order of 3–6 km. The dip directions of the fault blocks in the sub-basins together with the dips of the normal faults switch across the accommodation zones (Fig. 1b).

### 2.1. Stratigraphy

The stratigraphy of the northwestern margin of the Red Sea consists of Precambrian crystalline basement (metavolcanics, metasediments and granitoid intrusives; Akaad and Noweir, 1980; Said, 1990) together with Mesozoic–Cenozoic pre-rift sediments and Late Oligocene–Miocene to Recent syn-rift sediments (Fig. 2). The basement contains strong fabrics (faults, fractures, shear zones and dykes) oriented WNW, NNW, NS and ENE (Fig. 3). The basement is unconformably overlain by a 500–700-m-thick section of pre-rift strata that ranges in age from the Late Cretaceous to the Middle Eocene (Fig. 2). The lower part of the pre-rift section is the 130 m massive — thick-bedded, siliciclastic Nubia Formation. This is overlain by a 220–370-m-thick sequence of interbedded shales, sandstones and limestones of the Quseir, Duwi, Dakhla and Esna Formations (Fig. 2; Youssef, 1957; Abd El-Razik, 1967; Issawi et al., 1969). The uppermost pre-rift strata consist of 130–200 m of competent, thick-bedded limestones and cherty limestones of the Lower to Middle Eocene Thebes Formation (Fig. 2).

The Late Oligocene to Recent syn-rift strata unconformably overlie the Thebes Formation and vary in thickness from less than 100 m onshore to as much as 5 km in offshore basins (Heath et al., 1998). The lowermost syn-rift strata are dominantly coarse-grained clastics (Nakheil and Ranga Formations; Fig. 2). Overlying these clastics are reef limestones, clastics and evaporites (Um Mahara, Sayateen and Abu Dabbab Formations; Fig. 2). Late Miocene carbonates and reefs and Pliocene to Recent syn-rift clastics overlie the evaporites in the coastal outcrops (Figs. 2 and 3; Montenat et al., 1998; Plaziat et al., 1998).

### 2.2. Structure

The structure of the study area is dominated by two large, linked normal fault systems — the Border fault system and the Coastal fault system (Fig. 3a), and includes part of the Duwi accommodation zone (DAZ in Fig. 1b). This accommodation zone appears to have been localised by the Precambrian Hamrawin shear zone (Moustafa, 1997; Younes and McClay, 2001; Fig. 3a). In the northern part of the map area, the major faults dip to the northeast. South of the prominent Precambrian Hamrawin shear zone (Fig. 3a), the fault polarities change and the fault dip is mainly to the southwest (Fig. 3b). The Coastal fault system dominantly trends NW and delineates the main exposures of syn-rift strata along the Red Sea coast (Fig. 3a). Here the Anz fault segment (AF in Fig. 3a) dips NE but to the south, across the accommodation zone, the Zug el Bahar fault

segment dips SW (ZF in Fig. 3a). Minimum throws on the Coastal fault system vary from 0.5 to 2 km (based on topographic offset of basement and pre-rift strata).

The Border fault system is more complex. North and west of the Hamrawin shear zone it consists of the NE-dipping Kallahin fault (KF in Fig. 3a). South of the Hamrawin shear zone the Border fault system dips to the SW and is strongly segmented with two dominant faults — the Nakheil fault (NF in Fig. 3a) and the Hamadat fault (HF in Fig. 3a). Both of these faults exhibit three major strike directions — WNW, NW and N (Fig. 3a) — and typically display a zig-zag pattern. The hanging-wall structure of the Border fault system is characterised by several large, doubly-plunging, asymmetric hanging-wall synclines, the largest of which, the Gebel Duwi structure, is over 40 km long (Fig. 3a). The hanging-wall of the Hamadat fault also displays three prominent, but smaller, doubly-plunging synclines (Fig. 3a). In the immediate hanging-wall of the Border fault system, the beds dip steeply sub-parallel to the fault (Fig. 3b). Rare isolated outcrops of Late Oligocene syn-rift Nakheil sediments are found in the core of the Duwi structure (Fig. 3a and b). In the map area the estimated stratigraphic throw along the Border fault system varies from 1.5 to 3.5 km (based on topographic offset against basement and offsets of the pre-rift strata).

Cross-sections through the Duwi and Hamadat areas show that the Border fault system bounds a series of WNW- and NW-trending half grabens whose average width is 8 km and average bed dip is 15° towards the northeast (Fig. 3b). The half grabens are cut by smaller displacement faults into 1–3-km-wide, domino-style fault blocks. These smaller faults dip 55–65° and have stratigraphic throws that range from tens to a few hundreds of metres (Fig. 3b).

## 3. Extensional fault-related folding

### 3.1. Duwi Area

The Duwi map area is dominated by the massive outcrops of the Eocene Thebes limestone that form parts of the large complex, asymmetric syncline systems of the hanging wall of the Nakheil fault system (Fig. 4). The footwall of the Nakheil fault system consists dominantly of Precambrian basement (including the Hamrawin granite; Fig. 4a) except in the southern sections where gentle, moderately east-dipping Nubia sandstones occur in the footwall (Fig. 4b). Although the overall strike of the Nakheil fault system is NW, in detail the fault system is strongly segmented with NW-, WNW- and NS-striking sections (Fig. 4a). These dip 58–66° SW and have minimum stratigraphic offsets of 1.5–2.3 km. There are two distinct relay ramps (using the terminology of Larsen, 1988; Peacock and Sanderson, 1991; Peacock et al., 2000) that link what appear to be originally separate segments of the Naheil fault system (Fig. 4a). Relay R1 occurs along the margin of the Hamrawin granite body and relay R2 links the southern segments of the fault system (Fig. 4a). Fig. 5 shows the fault-displacement profiles for the Khalahin and Nakheil fault systems calculated using both stratigraphic and topographic offsets (note that these are minimum offsets as in most places the footwall stratigraphy has been removed by erosion). The relays and accommodation structures are developed at displacement minima on the fault profiles (Fig. 5). Relays R1 and R2 appear to be breached relays (cf. terminology of Childs et al., 1995).

There are four distinct, offset, NW-trending, hanging-wall synclines in the Duwi area (Fig. 4a). The northernmost, SE-plunging syncline is outlined by the massive outcrops of Thebes limestones and occurs in the hanging wall of the NE-dipping Kallahin fault, in the zone of transfer between it and the SW-dipping Nakheil fault system (Fig. 4a). The main northern Nakheil syncline is some 23 km long and has a curvilinear axial-surface trace, merging with the Kallahin syncline at its northwestern end (Fig. 4a). Its southern termination is a complex of en échelon normal faults where the syncline plunges gently to the north. The axial trace of the northern syncline has two bends localised by the Hamrawin granite and the relay ramp R1 (Fig. 4a). The doubly-plunging, central and southern Nakheil hanging-wall synclines are associated with separate NW- and N-trending Nakheil fault segments (Fig. 4a). The central and southern synclines are offset through a NS-trending fault that cuts across Wadi El Nakheil (Fig. 4a). The Nakheil synclines are noticeably asymmetric with gently (12–19°) E- and NE- dipping limbs and steep (30–60°) W–SW-dipping limbs (Fig. 4b). The E–NE-dipping limbs decrease in dip to only 7–9° further westwards away from the influence of the Nakheil fault. The panels of W–SW-dipping strata vary from 0.5 to 2 km in width. The width of the steep limb adjacent to the fault decreases with depth and appears to be absent at the top of the Precambrian basement and Nubia sandstones. Where the faults cut through basement and the massive to thick-bedded Nubia sandstones, footwall and hanging-wall deformation is localised to a few metres either side of the fault and no significant footwall or hanging wall folding is found. The NE–SW-oriented cross-sections show that the structural relief of the northern and central synclines is about 2 km and the wavelength is 5–6 km. Stereographic plots of poles to bedding (Fig. 6) show strong scattering typical of non-cylindrical fold systems with both N- and SSE-plunging fold axes. The double plunges (cf. Fig. 6) and basin shapes of individual synclines (Fig. 4a) can be directly correlated with the along-strike displacement variations of individual segments of the Nakheil fault system (cf. Fig. 5).

### 3.2. Hamadat area

The Hamadat area displays three well-exposed, doubly-plunging hanging-wall synclines bounded by distinct

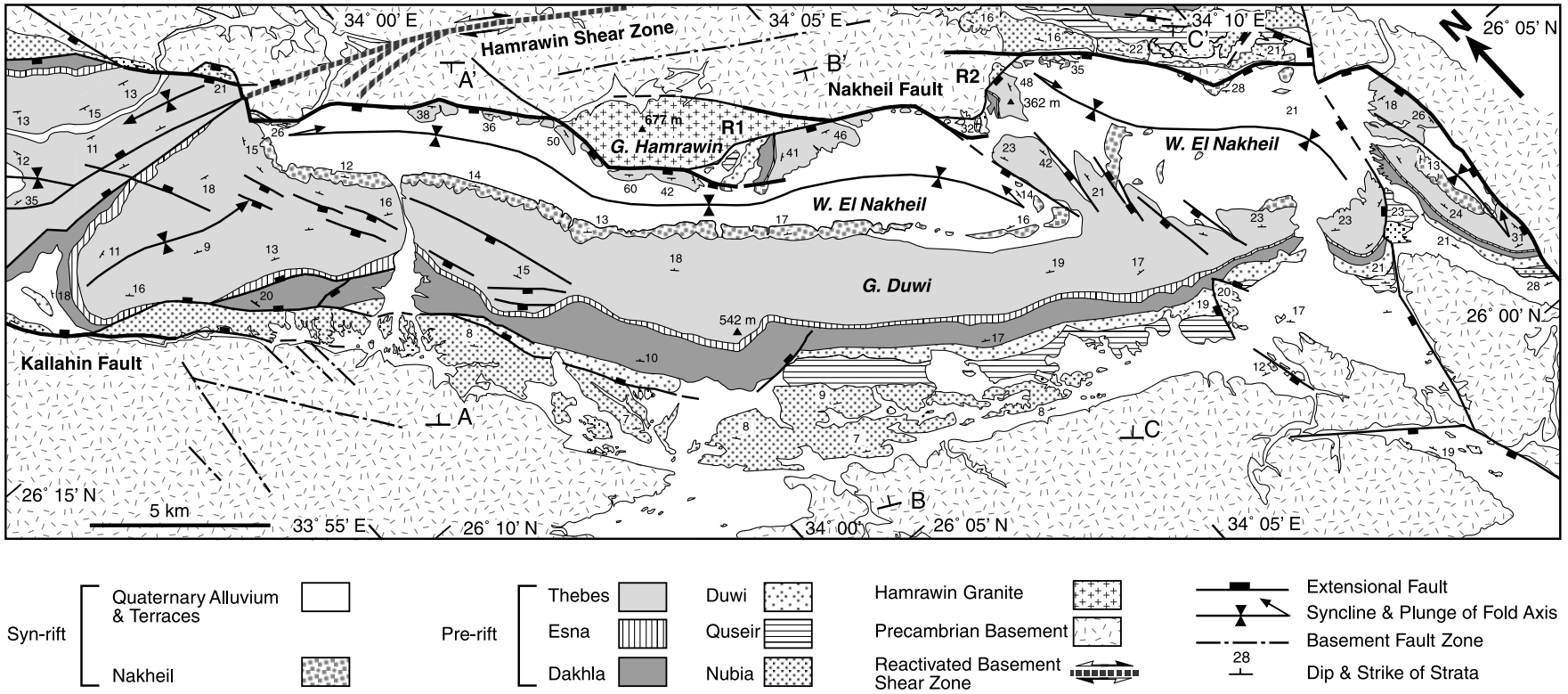


Fig. 4. (a) Detailed geologic map of Gebel Duwi area. (b) Structural cross-sections across the Gebel Duwi area (locations are shown in (a)).

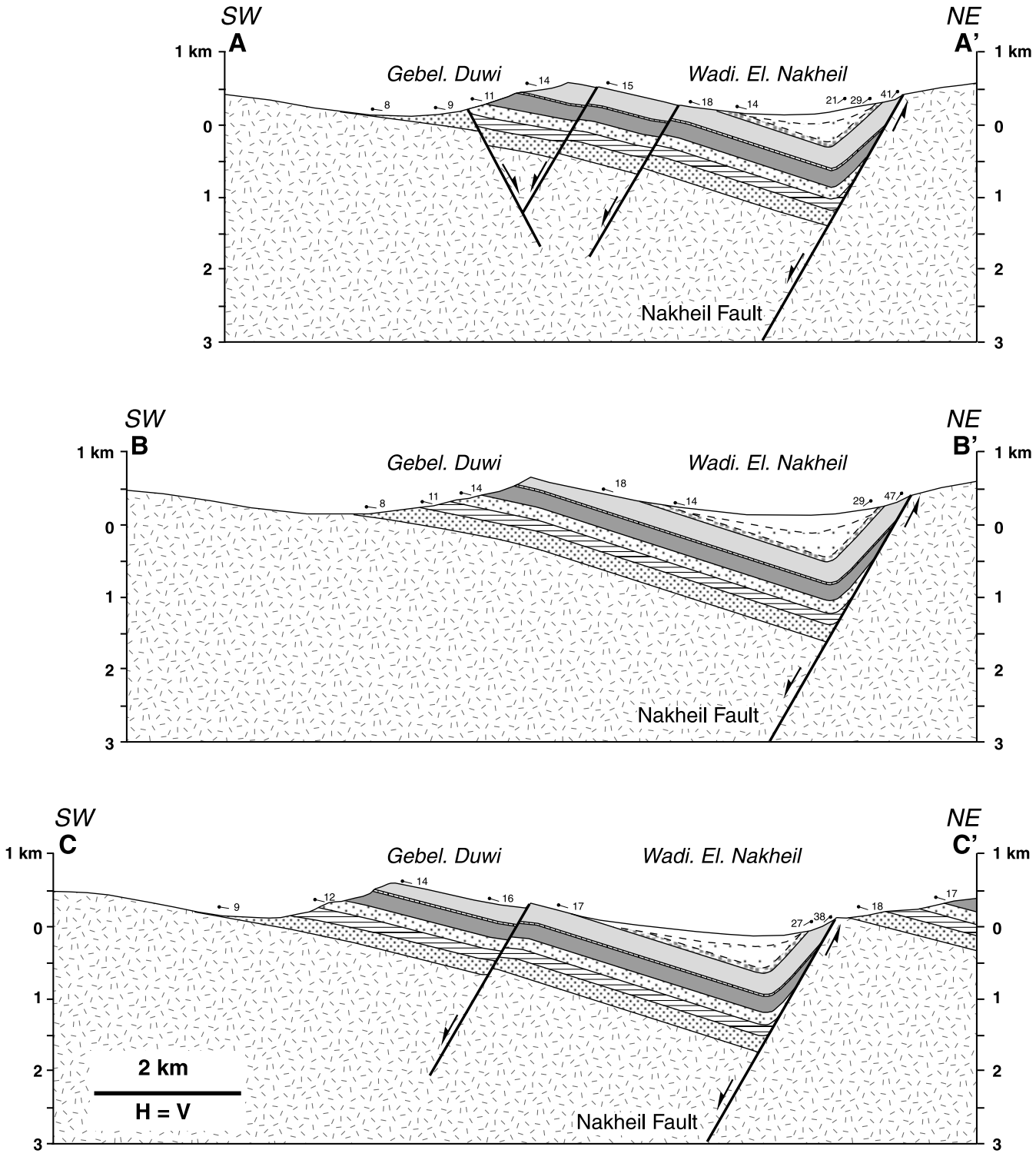


Fig. 4. (*continued*)

sections of the Hamadat fault (Fig. 7a). Here the Hamadat fault consists of two southern segments that trend NW, with each segment having a small individual hanging-wall syncline, and two northern, N-trending segments, one of which bounds the larger Hamadat syncline (Fig. 7a). Fault dips are typically 55–60° SW. Precambrian basement forms the footwall to all segments of the Hamadat fault. Stratigraphic offsets vary significantly along the strike of individual fault segments (cf. Fig. 7b) giving rise to the doubly-plunging, basin-shaped synclines with syncline axial traces sub-parallel to the fault segments (Fig. 7a). Calculations of greatest fault offsets in the central sections of each fault

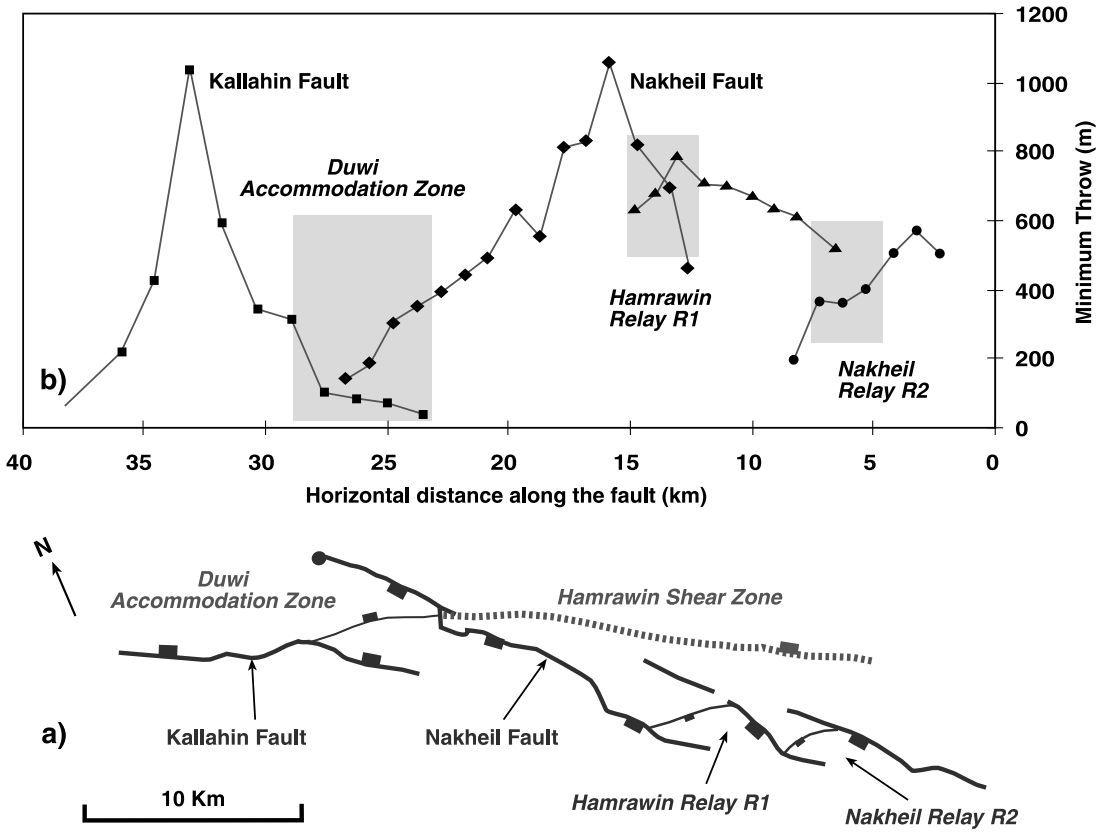


Fig. 5. (a) Simplified fault map for the Nakheil fault showing along-strike fault linkages, the Precambrian Hamrawin shear zone, the Khallahin fault and the Duwi accommodation zone. (b) Fault displacement profile along the Nakheil fault showing minimum fault displacements based on present day topography. Note that these are minimum throws as in most places erosion has removed all of the pre-rift strata in the footwall (data courtesy of A. Younes, pers. comm., 1998).

segment give 1.6 km for the northern syncline, 0.9 km for the central syncline and 1.2 km for the southern syncline. Note that these are minimum values as the pre-rift strata are eroded from the footwalls of the fault segments (Fig. 7). For the northernmost Hamadat syncline (Fig. 7a) the maximum fold amplitude of the fold is about 1.5 km and the wavelength is 4.5 km (cross-section B–B′; Fig. 7b). For the central and southern Hamadat synclines (Fig. 7a), the fold

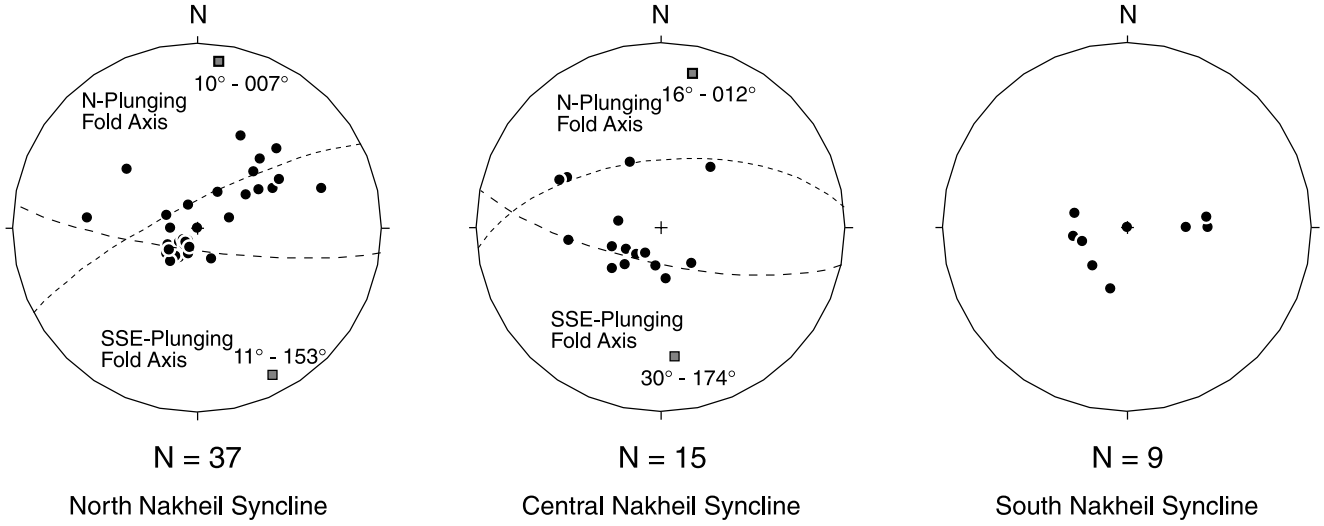


Fig. 6. Lower hemisphere equal area stereoplot of bedding in the three main hanging-wall synclines along Wadi El Nakheil. Where there was sufficient data, each syncline was divided into a north-plunging and south-plunging sub-area in order to determine the mean fold axis orientation.

amplitudes are 800 and 900 m, and the wavelengths are 2.2 and 3.2 km, respectively. Between the synclines there are two distinct but narrow, transverse anticlines (terminology of Schlische, 1995; Fig. 7a). These are located at the link points between originally separate segments of the Hamadat fault. These are points of minimum fault offset as indicated by the outcrops of the basal pre-rift Nubia sandstones in the immediate fault hanging walls.

In cross-section the Hamadat synclines are strongly asymmetric with long, gently NE-dipping limbs and short, steeply W- and SW-dipping limbs (Fig. 7). In the immediate hanging wall to the Hamadat fault, the steeply dipping (35–56°) panels of pre-rift strata vary from 0.4 to 0.8 km wide. In this steep NW-dipping limb, the shales of the Dakhla and Esna formations are thinned from an average total thickness of 150 m to only 60 m. Isolated outcrops of syn-rift Nakheil formation occur in the core of the north Hamadat syncline (Fig. 7). Stereographic plots (Fig. 8) show that the poles to bedding are strongly scattered, reflecting both the NW and SE trends of the doubly-plunging synclines, with the SE plunges (22–28°) being slightly greater than the NW plunges (10–16°).

## 4. Discussion

The excellent exposures in the Duwi and Hamadat areas show in detail the 3D geometries of kilometric-scale, asymmetric, hanging-wall synclines associated with major normal faults along the northwest Red Sea rift margin (Figs. 4 and 7). They are characterised by doubly-plunging, basin-like geometries, offset in an en échelon pattern and elongate sub-parallel to the Border fault system. In particular, the folds are characterised by steep SW-dipping limbs that dip in the same direction and are adjacent to the Border fault system (Figs. 4b and 7b). The kinked or rhomboidal pattern of the Border fault system (Fig. 3) together with the identification of breached relay ramps (Fig. 4a) and along-strike variations in fault displacements (Fig. 5) indicate that this fault system was initially strongly segmented. The development of a number of individual and en échelon offset hanging-wall synclines along the Duwi and Hamadat fault system is attributed to this initial fault segmentation (cf. Schlische, 1995). Displacement variations along individual fault segments (Fig. 5) gave rise to the periclinal double plunges of the asymmetric folds. Between the fault segments and the individual hanging-wall synclines are local highs and transverse anticlines (Fig. 7a). With continued extension during rifting, along-strike fault propagation leads to breaching of relay ramps (cf. Childs et al., 1995) and fault linkage (Trudgill and Cartwright, 1994; Dawers and Anders, 1995; Gupta and Scholz, 2000) producing the present-day fault pattern (Figs. 4a and 7a).

The kilometric-scale hanging-wall synclines of the Duwi and Hamadat areas are not typical rollover structures that are associated with listric normal faults (cf. Gibbs, 1984; McClay, 1990). Previous interpretations attributed the Duwi and Hamadat folds to strike-slip motion on the bounding faults (Jarrige et al., 1986; Montenat et al., 1988, 1998). No field evidence for strike-slip or oblique-slip normal faulting was found in this study. The en échelon nature of some of the initial fault segments of the Border fault system is attributed to N60°E regional extension, which was oblique to the reactivated basement fault zones, thus producing a pattern of en échelon offsets as observed in analogue models of oblique rifting (McClay, 1990). The extension-related hanging-wall folds were therefore also offset, controlled by the original extensional fault segmentation pattern.

Rift faults in the Gulf of Suez and the northwestern Red Sea exhibit essentially planar domino geometries (cf. Bosworth, 1995;Patton et al., 1994; Moustafa, 1997; Heath et al., 1998; McClay et al., 1998; Khalil and McClay, 2001; Younes and McClay, 2001). This, together with a lack of field evidence of steepening downwards fault systems, precludes a simple convex-up, extensional fault-bend fold, ramp-syncline model (cf. McClay and Scott, 1991; Suppe 1983) for the longitudinal hanging-wall synclines in the Duwi and Hamadat areas. As these late Oligocene–Miocene age folds are developed in an already lithified and compacted Cretaceous–Eocene pre-rift sequence, compactional drape folding may be ruled out as the mechanism for their development. The size and shape of these hanging wall synclines do not correspond to the 'reverse drag' models of hanging-wall folds (cf. Hamblin, 1965; Barnett et al., 1987). They are also not compatible with 'normal drag' structures, which tend to be much smaller in scale (normally only a few metres to tens of metres in size and restricted to the immediate hanging walls and footwalls of normal faults; Twiss and Moores, 1992; Davis and Reynolds, 1996).

Our preferred interpretation for the development of these hanging-wall synclines is therefore that of extension-related fault-propagation folding along individual segments of the Border fault system. Tip-line or fault-propagation folding (also termed 'forced folding'; Stearns, 1978; see also review by Cosgrove and Ameen, 1999) has long been recognised as an important fault-related fold mechanism in thrust terranes (cf. Rich, 1934; Dahlstrom, 1970; Suppe, 1985; Jamison, 1987). It has received only relatively recent attention in extensional terranes (Allmendinger, 1998; Cosgrove and Ameen, 1999; Hardy and McClay, 1999; Corfield and Sharp, 2000; Sharp et al., 2000). It has, however, been recognised in regions where pre-extensional salt layers have influenced hanging-wall geometries (e.g. Withjack et al., 1989, 1990; Richard, 1991; Withjack and Callaway, 2000). In particular, few 3D descriptions of exposed examples of extension-related fault-propagation folds have been given (e.g. Gawthorpe et al., 1997; Maurin and Niviere, 1999; Sharp et al., 2000).

Extension-related fault-propagation folding (cf. Hardy and McClay, 1999) would produce hanging-wall synclines

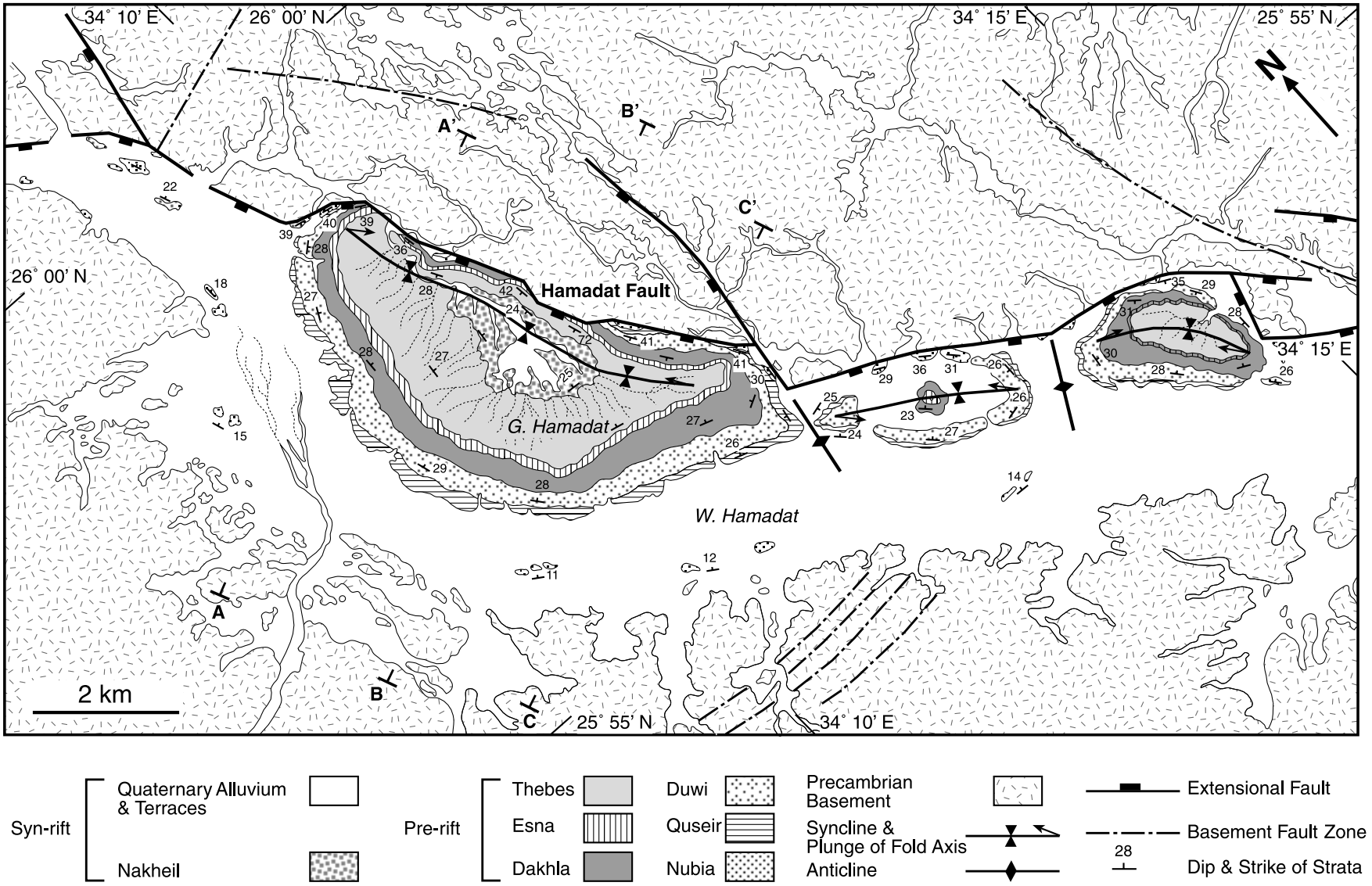


Fig. 7. (a) Detailed geological map of the Hamadat area showing the Hamadat fault and the doubly-plunging hanging-wall synclines along Wadi Hamadat. (b) Structural cross-sections across the main Gebel Hamadat area (locations are shown in (a)).

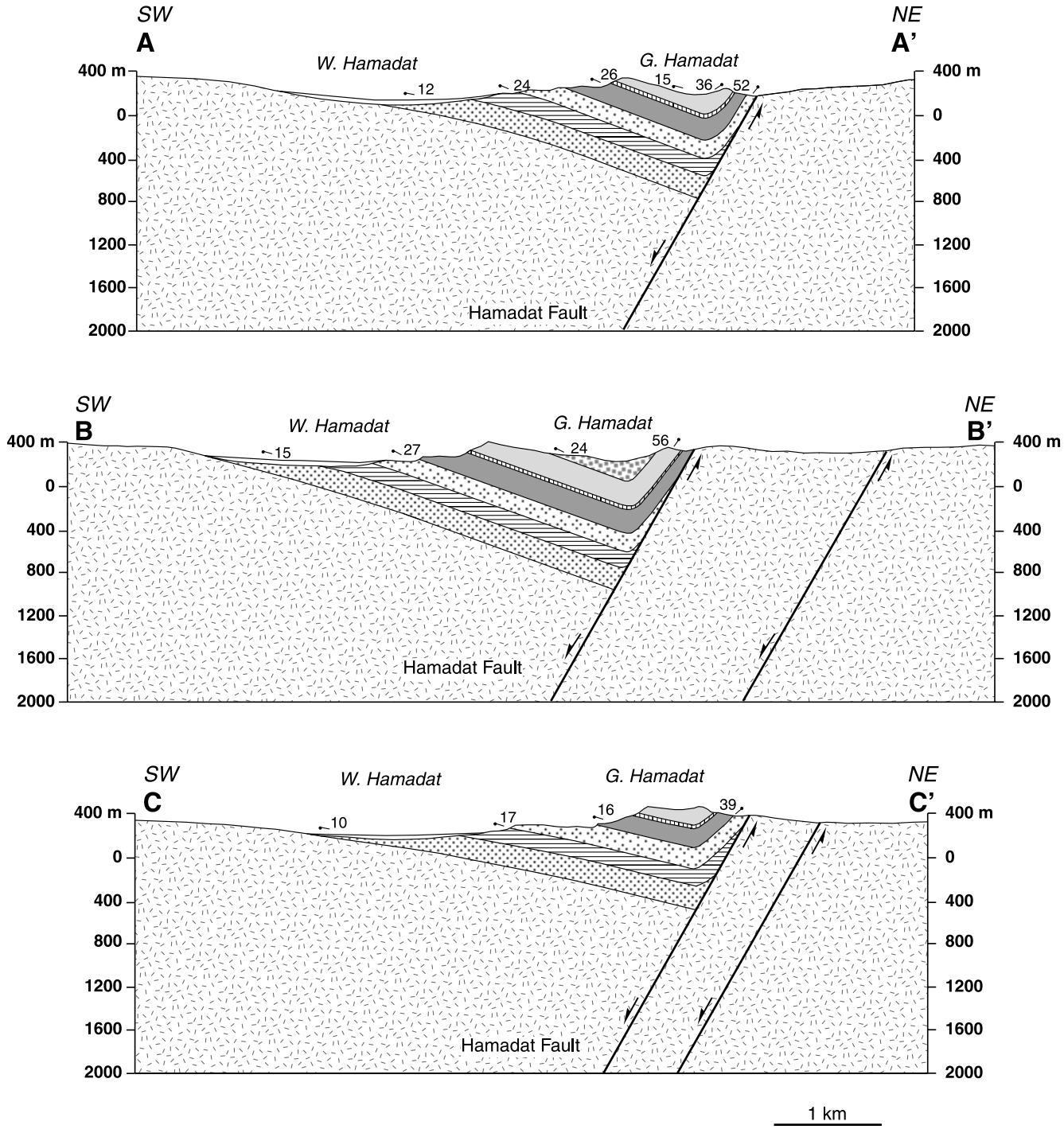


Fig. 7. (*continued*)

of the kind found in the Duwi and Hamadat areas (Figs. 4 and 7). In particular, the highly anisotropic nature of the Late Cretaceous units, namely the Queseir–Esna section with abundant shale units, noteably in the Dakhla and Esna formations (Fig. 2), would enhance flexural slip needed to accommodate fault-propagation folding (cf. Suppe, 1985). Outcrop studies in the Duwi and Hamadat areas reveal that the Dakhla formation in particular is commonly highly sheared with abundant gypsum veining in the proximity of the major faults (both in the footwall and in the hanging wall).

### *4.1. Trishear numerical modelling of extension-related fault-propagation folding*

In order to validate our interpretation of an extensional-fault propagation origin for these hanging-wall folds, a series of numerical models were constructed using

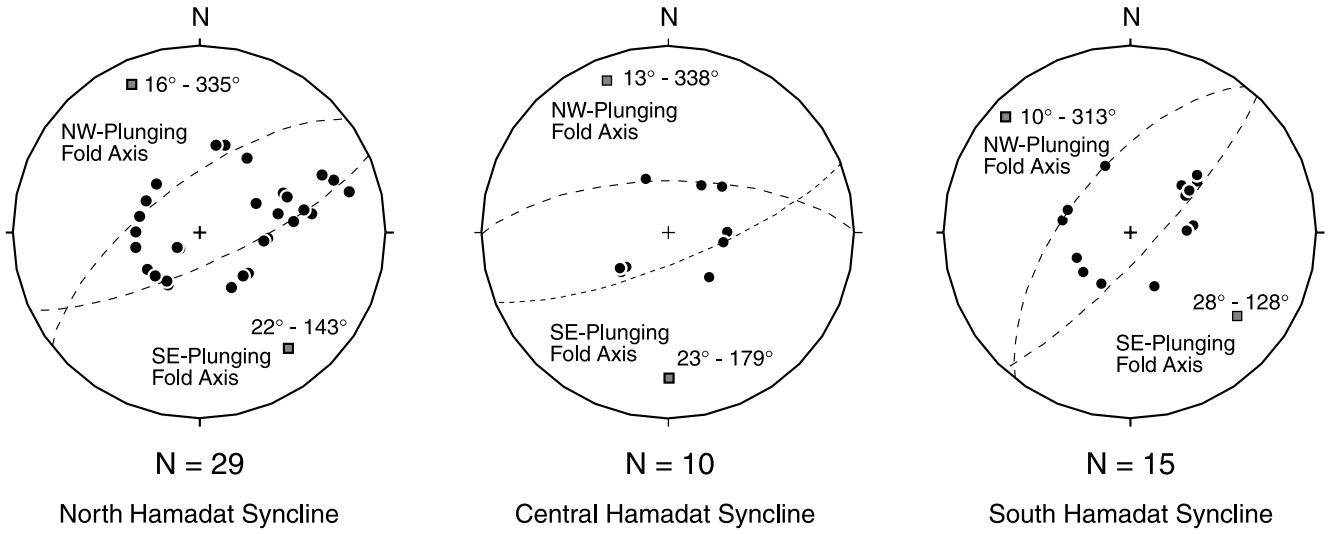


Fig. 8. Lower hemisphere equal area stereoplot of bedding in the three main hanging-wall synclines along Wadi Hamadat. Where there was sufficient data each syncline was divided into a north-plunging and a south-plunging sub-area in order to determine the mean fold axis orientation.

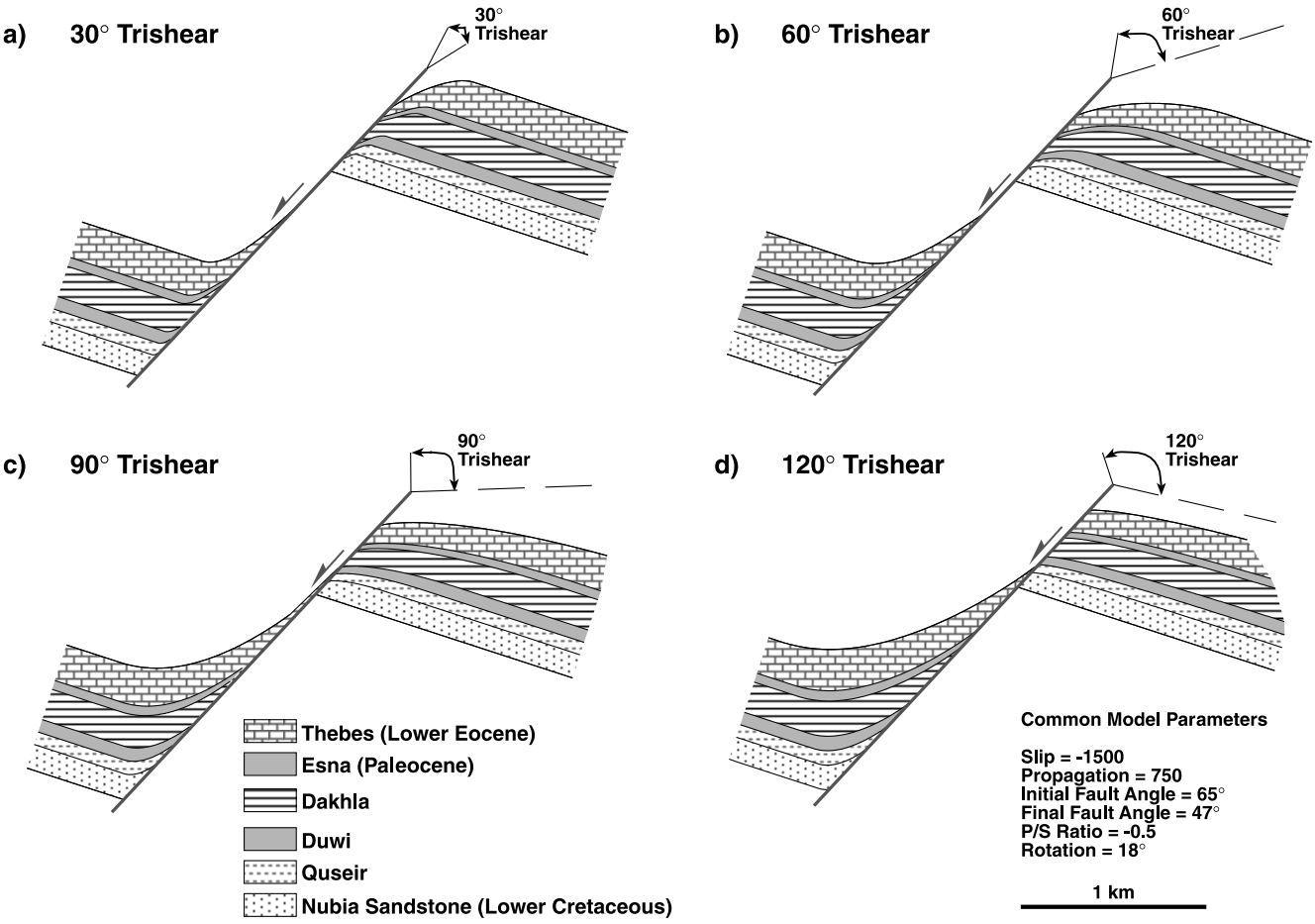


Fig. 9. Numerical models of extensional fault-propagation folds simulated using the *Trishear* program (Allmendinger, 1998). The initial stratigraphic template was constructed using the mean thicknesses for the pre-rift succession in the northwestern Red Sea rift margin. Results of four models with different trishear angles. Initial fault dip 65°. Total fault slip 1500 m. Fault propagation to slip ratio −0.5. Total rotation 18°. Initial position of fault at base of pre-rift Nubia section. (a) Trishear angle = 30°; (b) Trishear angle = 60°; (c) Trishear angle = 90°; (d) Trishear angle = 120°.

Allmendinger's *Trishear* modelling program (Allmendinger, 1998). Trishear deformation was first proposed by Erslev (1991) and then developed by Hardy and Ford (1997), Allmendinger (1998) and Hardy and McClay (1999) to numerically model fault-propagation folding. In the trishear model, fault-propagation folding is achieved by deformation in an outwardly-widening triangular zone of simple shear emanating from the fault tip, which also moves through the stratigraphy as the fault propagates up-section. The resultant fault-propagation fold is a function of the angle of trishear, the total fault slip $S$, and the ratio of fault propagation $P$ to the fault slip $S$ (Allmendinger, 1998). We have applied this modelling method to simulate 2D fault-propagation folding above an upward-propagating normal fault. For these models, an initial fault dip of 65° was chosen with the initial tip of the fault located at the top of the basement and below the basal pre-rift succession. In this way the models attempt to simulate the reactivation of a pre-existing fault in the basement. The pre-deformational template above the initial fault tip was constructed using mean values for the pre-rift stratigraphy (note that the numerical models are purely geometric and there is no mechanical stratigraphy). Total fault displacement of 1500 m and a total rigid block rotation of 18° was chosen in order to approximate the finite fault-block geometries in the Duwi and Hamadat areas.

Fig. 9 shows the end results of four extensional fault-propagation models with trishear angles that vary from 30 to 120° and a constant $P/S$ ratio of $-0.5$. With increased angle of trishear the amount of footwall folding is reduced and the width of the hanging-wall syncline increases (Fig. 9). For a 120° trishear angle, there is very little footwall deformation and a broad hanging-wall syncline with a substantial panel of strata dipping steeply in the same direction as the fault. As the fault-propagation folding is accommodated by bed-parallel slip, a trishear angle of 120°, which has one of the boundaries of the trishear zone sub-parallel to the bedding in the footwall block (Fig. 9d), simulates the development of layer-parallel flexural-slip deformation in this block. This is considered to be a close approximation to the intense layer-parallel shearing observed in the field in the shale units — particularly in the Dakhla and Esna formations. Fig. 10 shows the results of 120° trishear models where the $P/S$ ratio was varied from $-1.0$ (fault slip = fault propagation) to $-0.1$, (where the fault only propagates one tenth of the slip value). With a decrease in the $P/S$ ratio the amount of hanging-wall folding increases until at $P/S$ ratios of $-0.1$ the fault tip does not propagate beyond the base of the Duwi formation. Folding is accommodated by layer-parallel slip and thinning of units in the hanging wall (Fig. 10). Fig. 11 shows the progressive evolution of our preferred model that approximates many of the features seen in the natural extensional fault-related folds with little footwall deformation and a wide hanging wall syncline that compares closely with the Duwi and Hamadat folds (cf. Figs. 4b and 7b). Note that in the natural cross-sections (Figs. 4b and 7b; (and in the numerical models), the Duwi–Esna section is strongly thinned in the hanging wall with increased in-line length compared with the basal Nubia section.

In 3D the along-strike map patterns (Figs. 4a and 7a) show that the offset hanging-wall synclines are related to individual segments of the normal fault system. Along-strike displacement variations (cf. Fig. 5) give rise to the double plunges observed in the field and on the maps. Fig. 12 shows a conceptual kinematic model for the 3D evolution of the Duwi folds. Initial N60°E-directed extension reactivated NW-trending basement fault zones producing isolated, asymmetric synclines at the surface (top of the pre-rift sequence; Fig. 12a). Continued extension produced upward fault propagation such that surface breakthrough occurred (Fig. 12b). The steep limbs of the synclines were cut by the normal faults, producing a hanging-wall panel that dips steeply in the same direction as the fault. With continued extension (stages II and IV, Fig. 12c and d), along-strike propagation of the individual fault segments produced linkage and relay ramps that became breached. Transverse folds and elevated zones formed at the points of segment linkage and at the breached relay ramps (cf. Fig. 7a). Continued slip on the linked fault system produced larger, linked hanging wall synclines (cf. the long north Duwi syncline; Fig. 4a). Syn-extensional sedimentation would have been focused along the longitudinal axes of the hanging-wall synclines, whereas footwall uplift would have produced erosion of the pre-rift strata (Fig. 12d).

The kinematic model proposed in Fig. 12 accounts both for the longitudinal plunge variations of the hanging-wall synclines as well as the extensional fault-propagation features of these structures. A similar model may also be applied to the Hamadat synclines where probably both NW- and NS-trending, pre-existing basement fault zones were reactivated during the Late Oligocene–Miocene extension.

Kilometric-scale, extension-related, hanging-wall fault-propagation folds have been described in similar pre-rift sequences on the eastern Gulf of Suez rift margin (Moustafa, 1987; Patton et al., 1994; Gawthorpe et al., 1997; Sharp et al., 2000). There they clearly influenced and played an important role in the dispersal of syn-rift sediments and on syn-rift stratal architectures (Gupta et al., 1999; Sharp et al., 2000). Extension-related fault-propagation folds also have been described for structures in the North Sea and offshore Norway (Corfield and Sharp, 2000) and for fold structures in the Rhine Graben (Maurin and Niviere, 1999).

## 5. Conclusions

Detailed field mapping and analysis has demonstrated that the kilometric-scale, doubly-plunging, asymmetric hanging-wall synclines of the Duwi and Hamadat areas

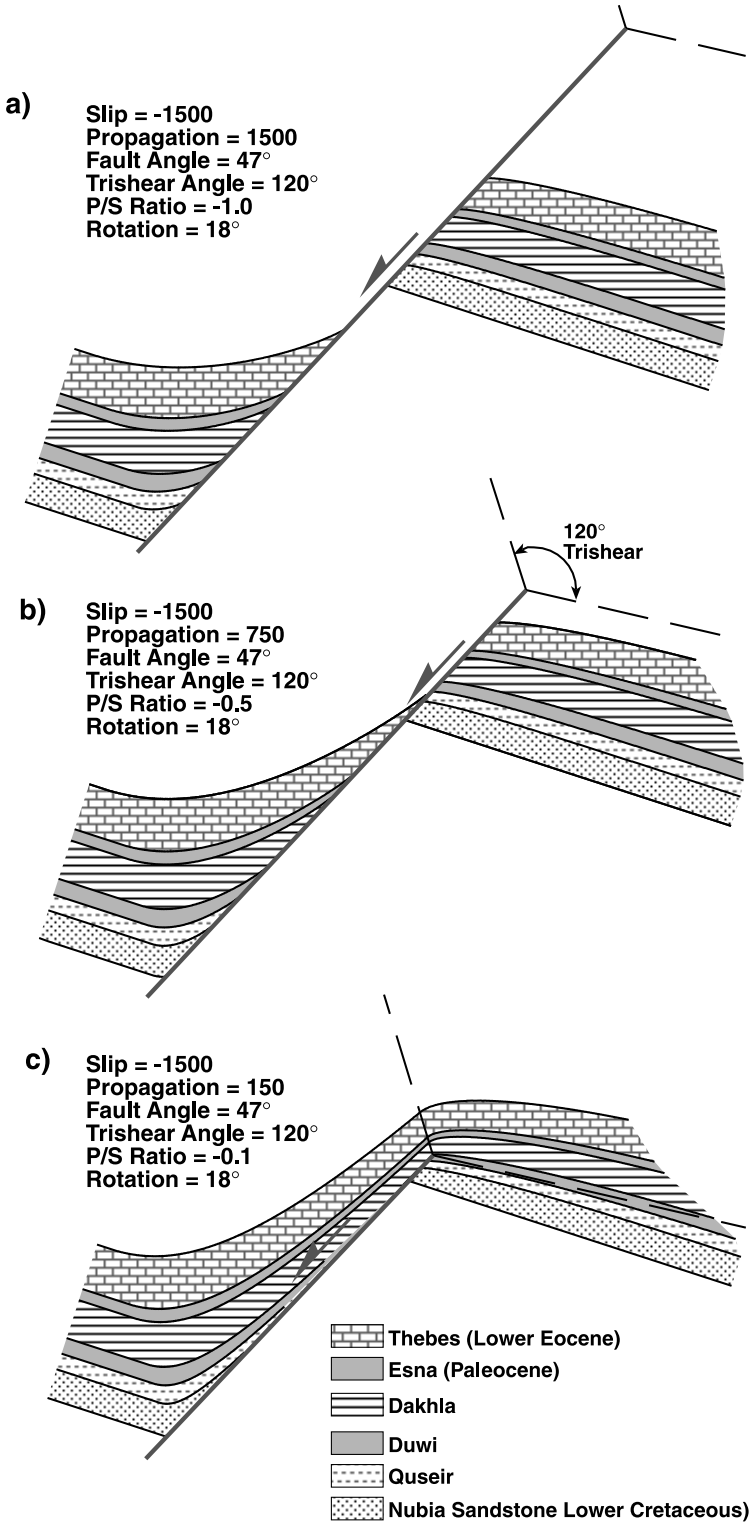


Fig. 10. Numerical models of extensional fault-propagation folds simulated using the *Trishear* program (Allmendinger, 1998). The initial stratigraphic template was constructed using the mean thicknesses for the pre-rift succession in the northwestern Red Sea rift margin. Results of three models for 120° trishear angle, but with different fault propagation (*P*) to fault slip (*S*) ratios. Initial fault dip 65°. Total fault slip 1500 m. Trishear angle 120°. Total rotation 18°. Initial position of fault at base of pre-rift Nubia section. (a) *P*/*S* ratio = −1.0; (b) *P*/*S* ratio = −0.5; (c) *P*/*S* ratio = −0.1.

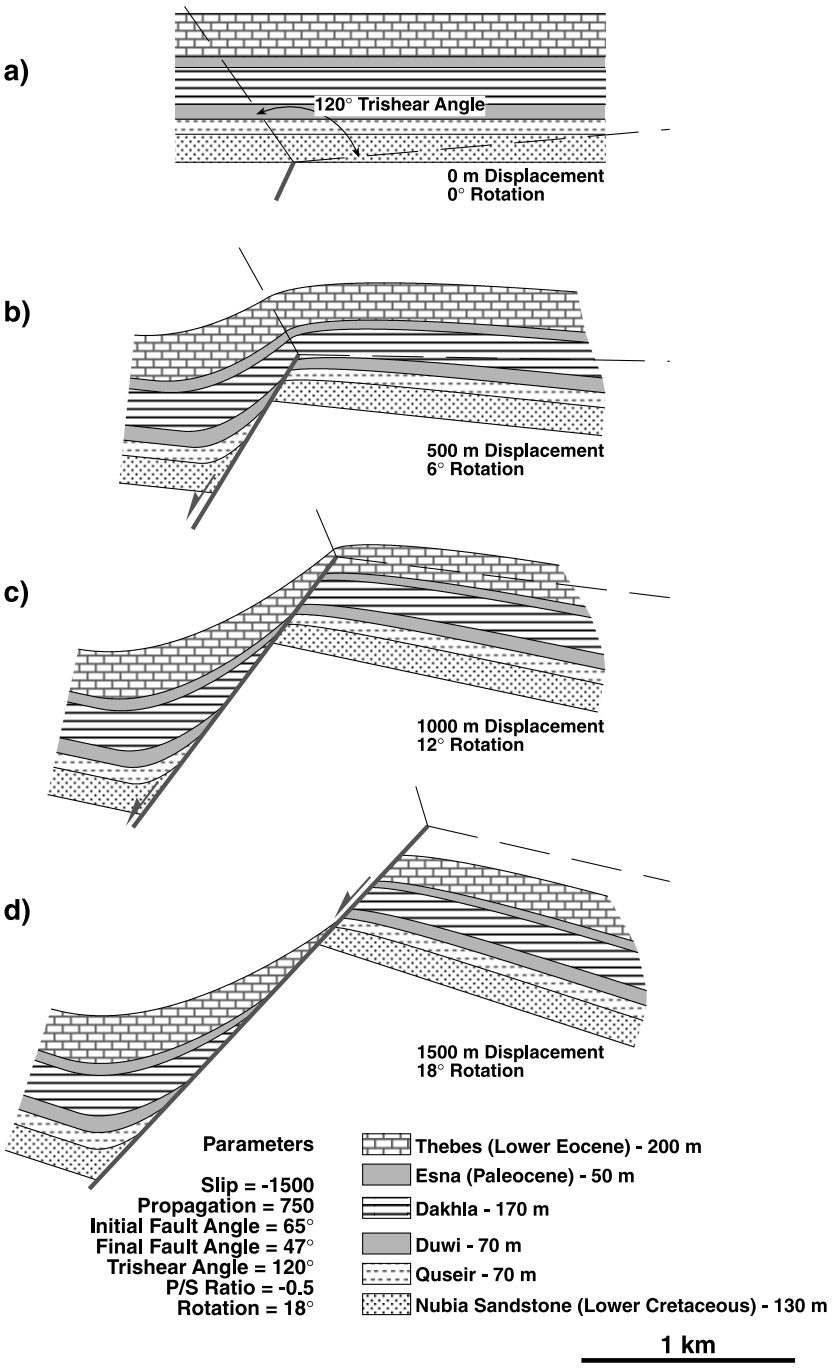


Fig. 11. Numerical models of extensional fault-propagation folds simulated using the *Trishear* program (Allmendinger, 1998). The initial stratigraphic template was constructed using the mean thicknesses for the pre-rift succession in the northwestern Red Sea rift margin. Progressive evolution of the preferred model with a trishear angle of 120°. Initial fault dip 65°. Total fault slip 1500 m. Fault propagation to slip ratio = −0.5. Total rotation 18°. Initial position of fault at base of pre-rift Nubia section. (a) Initial state; (b) after a fault slip of 500 m; (c) after a fault slip of 1000 m; (d) after a fault slip of 1500 m.

are large extension-related, fault-propagation folds formed in anisotropic pre-rift strata during Late Oligocene–Miocene extension of the Red Sea rift. Separate offset synclines were formed in the hanging walls of individual NW- and N–S-trending segments of the rift Border fault system. Continued extension produced along-strike linkage of the fault system and formation of the large, asymmetric, hanging-wall synclines that are observed today. Along-strike plunge changes are a result of displacement variations on the bounding normal fault segments. Numerical simulations using the trishear model show how these hanging-wall synclines may have formed by extensional fault-propagation folding. The models successfully replicate the Duwi and Hamadat fold geometries and dimensions in 2D. Bed-parallel flexural slip and thinning of anisotropic shale layers in the pre-rift sequence is an important accommodation

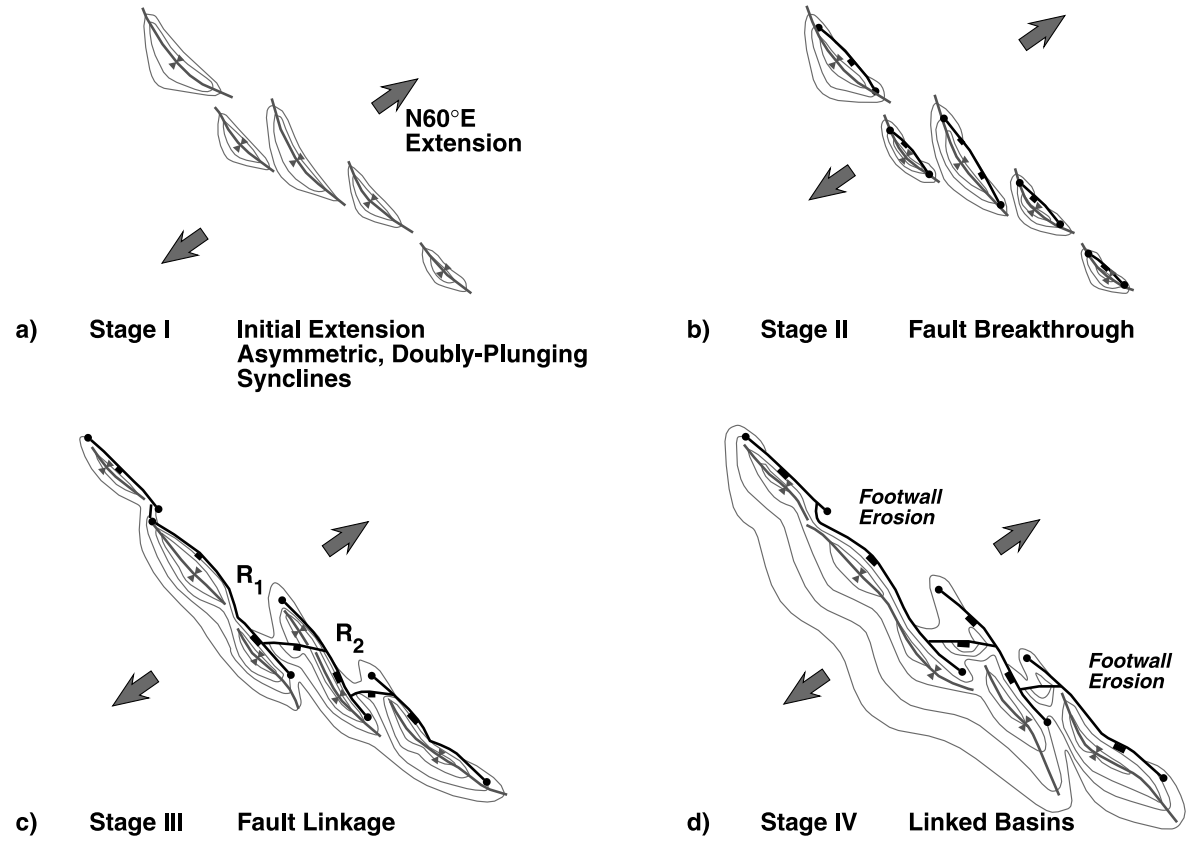


Fig. 12. Conceptual kinematic model for the progressive evolution of extensional fault-related folds in the Duwi area. (a) Isolated asymmetric synclines, offset in an en échelon pattern. (b) Surface breakthrough of segmented normal faults offsetting the syncline limbs. (c) Linkage of normal fault segments by along-strike propagation and breaching of relay ramps. (d) Continued extension on linked normal fault system with along-stike linkage of hanging-wall synclines.

mechanism that permits these hanging-wall synclines to develop. The Duwi and Hamadat folds compare closely in size and characteristics with similar extension-related fault-propagation folds described by other authors from the eastern Gulf of Suez and offshore Norway.

## Acknowledgements

This research was supported by the Natural Environment Research Council ROPA Grant GR3/R9529. Additional support from the Fault Dynamics Project (sponsored by ARCO British Limited, PETROBRAS UK. Ltd, BP Exploration, Conoco (UK) Limited, Mobil North Sea Limited, and Sun Oil Britain). K. McClay also gratefully acknowledges support from ARCO British Limited and BP Exploration. Bill Bosworth and Marathon Petroleum Egypt are thanked for logistical support. Bill Bosworth and Amgad Younes are thanked for many fruitful discussions on the geology of the northwestern Red Sea. S. Khalil was supported by a Research Grant to KMcC. from BG International. BG Egypt and Maher Ayyad kindly assisted with additional fieldwork in the northwestern Red Sea. T. Dooley kindly assisted with the numerical modelling and diagram preparation. R. Allmendinger (Cornell) is gratefully acknowledged for allowing us to use his *Trishear*numerical modelling program. Fault Dynamics Publication No. 104. Critical reviews by D. Peacock, T. Apotria, N. Dawers and D. Waltham were greatly appreciated.

## References

Abd El-Razik, T.M., 1967. Stratigraphy of the sedimentary cover of the Anz–Atshan–south Duwi district. Bulletin of the Faculty of Science, Cairo University 431, 135–179.

Akaad, M.K., Noweir, A.M., 1980. Geology and lithostratigraphy of the Arabian desert orogenic belt between latitudes 25°35′ and 26°30′. In: Cooray, P.A.T.S. (Ed.). Evolution and Mineralization of the Arabian-Nubian Shield 4. Permagon Press, New York, pp. 127–135.

Allmendinger, R.W., 1998. Inverse and forward numerical modelling of trishear fault-propagation folds. Tectonics 17, 640–656.

Barnett, J.A.M., Mortimer, J., Rippon, J.H., Walsh, J.J., Watterson, J., 1987. Displacement geometry in the volume containing a single normal fault. American Association of Petroleum Geologists Bulletin 71, 925–937.

Ben-Menahem, A., Nur, A., Vered, M., 1976. Tectonics, seismicity and structure of the Afro-Eurasian junction — the breaking of an incoherent plate. Physics of the Earth Planetary Interiors 12, 1–50.

Bosworth, W., 1985. Geometry of propagating continental rifts. Nature 316, 625–627.

Bosworth, W., 1995. A high strain model for the southern Gulf of Suez (Egypt). In: Lambiase, J.J. (Ed.), Hydrocarbon Habitat in Rift Basins. Geological Society of London Special Publication 80, 75–102.

Bosworth, W., McClay, K.R., 2001. Structural and stratigraphic evolution

of the Neogene Gulf of Suez, Egypt: a synthesis. In: Cavazza, W., Robertson, A.H.F.R., Zeigler, P. (Eds.), 'Peritethyan Rift/Wrench Basins and Passive Margins'. Memoires due Museum National d'Historie Naturelle de Paris: Peritethys Programme (PTP) and IGCP 369 Special Publication, in press.

Childs, C., Watterson, J., Walsh, J.J., 1995. Fault overlap zones within developing normal fault systems. Journal Geological Society of London 152, 535–549.

Coffield, D.Q., Schamel, S., 1989. Surface expression of an accommodation zone within the Gulf of Suez rift, Egypt. Geology 17, 76–79.

Corfield, S., Sharp, I.R., 2000. Structural style and stratigraphic architecture of fault propagation folding in extensional settings: a seismic example from the Smørbukk area, Halten Terrace, Mid-Norway . Journal of Basin Research 12, 329–341.

Coleman, R.G., 1993. Geologic Evolution of the Red Sea. Oxford Monographs on Geology and Geophysics 24. Oxford University Press, Oxford, 186pp.

Cosgrove, J.W., Ameen, M.S., 1999. A comparison of the geometry, spatial organisation and fracture patterns associated with forced folds. In: Cosgrove, J.W., Ameen, M.S. (Eds.), Forced Folds and Fractures. Geological Society of London Special Publication 169, 7–21.

Dahlstrom, C.D.A., 1970. Structural geology in the eastern margin of the Canadian Rocky Mountains. Bulletin of Canadian Petroleum Geology 18, 332–406.

Davies, F.B., 1984. Strain analysis of wrench faults and collision tectonics of the Arabian-Nubia sheild. Journal of Geology 82, 37–53.

Davis, G.H., Reynolds, S.J., 1996. Structural Geology of Rocks and Regions. 2nd Ed John Wiley and Sons, Chichester.

Dawers, N.H., Anders, M.H., 1995. Displacement-length scaling and fault linkage. Journal of Structural Geology 17, 604–614.

Dixon, T.H., Stern, R.J., Hussein, I.M., 1987. Control of Red Sea rift geometry by Precambrian structures. Tectonics 5, 551–571.

Erslev, E.A., 1991. Trishear fault-propagation folding. Geology 19, 617–620.

Faulds, J.E., Varga, R.J., 1998. The role of accommodation zones and transfer zones in the regional segmentation of extended terranes. In: Faulds, J.E., Stewart, J.H. (Eds.), Accommodation Zones and Transfer Zones: the Regional Segmentation of the Basin and Range Province. Geological Society of America Special Publication 323, 1–45.

Freund, R., 1970. Plate tectonics of the Red Sea and Africa. Nature 228, 453.

Gawthorpe, R.L., Sharp, I., Underhill, J.R., Gupta, S., 1997. Linked sequence stratigraphic and structural evolution of propagating normal faults. Geology 25, 795–798.

Gibbs, A., 1984. Structural evolution of extensional basin margins. Journal of the Geological Society of London 141, 609–620.

Gupta, A., Scholz, C.H., 2000. A model of normal fault interaction based on observations and theory. Journal of Structural Geology 22, 856–879.

Gupta, S.H., Underhill, J.R., Sharp, I.R., Gawthrope, R.L., 1999. Role of fault interactions in controlling syn-rift dispersal patterns: Miocene, Abu Alaqa Group, Suez Rift, Sinai, Egypt. Basin Research 11, 167–189.

Hamblin, W.K., 1965. Origin of 'reverse drag' on the downthrow side of normal faults. Geological Society of America Bulletin 76, 1145–1164.

Hardy, S., Ford, M., 1997. Numerical modeling of trishear fault-propagation folding. Tectonics 16, 841–854.

Hardy, S., McClay, K.R., 1999. Kinematic modelling of extensional fault-propagation folding. Journal of Structural Geology 21, 695–702.

Heath, R., Vanstone, S., Swallow, J., Ayyad, M., Amin, M., Huggins, P., Swift, R., Warburton, I., McClay, K., Younis, A., 1998. Renewed exploration in the offshore north Red Sea Region, Egypt. Proceedings of the 14th Petroleum Conference, Egyptian General Petroleum Corporation, Cairo, Egypt, pp. 16–34.

Hempton, M., 1987. Constraints on Arabian plate motion and extensional history of the Red Sea. Tectonics 6, 687–705.

Issawi, B., Francis, M., El-Hinnawi, M., Mehanna, A., 1969. Contribution to the structure and phosphate deposits of Quseir area. Geological Survey of Egypt Paper, 50.

Jamison, W.R., 1987. Geometric analysis of fold development in overthrust terranes. Journal of Structural Geology 9, 207–219.

Janecke, S.U., Vandenburg, C.J., Blankenau, J.J., 1998. Geometry, mechanisms, and significance of extensional folds from examples in the Rocky Mountain Basin and Range province, USA. Journal of Structural Geology 20, 841–856.

Jarrige, J.J., Ott D'estevou, P., Burollet, P.F., Thiriet, J.P., Icart, J.C., Richet, J.P,, Sehans, P., Montenat, C., Prat, P., 1986. Inherited discontinuities and Neogene structure: the Gulf of Suez and the northwestern edge of the Red Sea. Philosophical Transactions of the Royal Society of London A 317, 129–139.

Keller, J.V.A., Lynch, G., 1999. Displacement transfer and forced folding in the Maritimes basin of Nova Scotia, Eastern Canada. In: Cosgrove, J.W., Ameen, M.S. (Eds.), Forced Folds and Fractures. Geological Society of London Special Publication 169, 87–101.

Khalil, S.M., McClay, K.R., 2001. Tectonic evolution of the northwestern Red Sea–Gulf of Suez rift system. In: Wilson, C.J, Whitmarsh, R. (Eds.), Non-Volcanic Rifted Margins, Geological Society of London Special Publication 187, in press.

Larsen, P.H., 1988. Relay structures in a Lower Permian basement-involved extension system, East Greenland. Journal of Structural Geology 10, 3–8.

Le Pichon, X., Francheteau, J., 1978. A plate tectonic analysis of the Red Sea–Gulf of Aden area. Tectonophysics 46, 369–406.

Maurin, J.-C., Niviere, B., 1999. Extensional forced folding and decollement of the pre-rift series along the Rhine graben and their influence on the geometry of the syn-rift sequences. In: Cosgrove, J.W., Ameen, M.S. (Eds), Forced Folds and Fractures, Special Publication. 169, 73–86.

McClay, K.R., 1990. Extensional fault systems in sedimentary basins: a review of analogue model studies. Marine and Petroleum Geology 7, 206–233.

McClay, K.R., Scott, A.D., 1991. Experimental models of hanging wall deformation in ramp-flat listric extensional fault systems. Tectonophysics 188, 85–96.

McClay, K.R., Nichols, G.J., Khalil, S., Darwish, M., Bosworth, W., 1998. Extensional tectonics and sedimentation, Eastern Gulf of Suez, Egypt. In: Purser, B., Bosence, D.W.J. (Eds.). Sedimentation and Tectonics of Rift Basins: Red Sea–Gulf of Aden. Chapman & Hall, London, pp. 223–238.

McKenzie, D.P., Davies, D., Molnar, P., 1970. Plate tectonics of the Red Sea and east Africa. Nature 226, 243–248.

Meshref, W.M., 1990. Tectonic framework. In: Said, R. (Ed.). The Geology of Egypt. Balkema, Rotterdam, pp. 113–155, Chapter 8.

Montenat, C., Ott D'estevou, P., Purser, B., Burollet, P., Jarrige, J., Sperber, F., Philobbos, E., Plaziat, J.-C., Prat, P., Richert, J., Roussel, N., Theiriet, J., 1988. Tectonic and sedimentary evolution of the Gulf of Suez and the northern western Red Sea. Tectonophysics 153, 166–177.

Montenat, C., Ott D'estevou, P., Jarrige, J.-J., Richert, J.-P., 1998. Rift development in the Gulf of Suez and the north-western Red Sea: structural aspects and related sedimentary processes. In: Purser, B.H., Bosence, D.W.J. (Eds.). Sedimentation and Tectonics of Rift Basins: Red Sea–Gulf of Aden. Chapman and Hall, London, pp. 97–116.

Morgan, P., 1990. Egypt in the tectonic framework of global tectonics. In: Said, R. (Ed.). The Geology of Egypt. Balkema, Rotterdam, pp. 91–111 Chapter 7.

Moustafa, A.M., 1976. Block faulting of the Gulf of Suez. Presented at 5th Exploration Seminar, Egyptian General Petroleum Company, Cairo, Unpublished Report, 19pp.

Moustafa, A.R., 1987. Drape folding in the Baba–Sidri area, eastern side of the Suez rift. Egyptian Journal of Geology 31, 15–27.

Moustafa, A.R., 1997. Controls on the development and evolution of transfer zones: the influence of basement structure and sedimentary thickness in the Suez rift and Red Sea. Journal of Structural Geology 6, 755–768.

Patton, T.L., Moustafa, A.R., Nelson, R.A., Abdine, S.A., 1994. Tectonic evolution and structural setting of the Suez rift. In: Landon, S.M. (Ed.), Interior Rift Basins. American Association of Petroleum Geologists Memoir 59, 9–55.

Peacock, D.C.P., Sanderson, D.J., 1991. Displacements, segment linkage and relay ramps in normal fault zones. Journal of Structural Geology 13, 721–733.

Peacock, D.C.P., Knipe, R.J., Sanderson, D.J., 2000. Glossary of normal faults. Journal of Structural Geology 22, 291–306.

Plaziat, J.-C., Baltzer, F., Choukri, A., Conchon, O., Freytet, P., Orszag-Sperber, F., Raguideau, A., Reyss, J.-L., 1998. Quaternary marine and continental sedimentation in the northern Red Sea and Gulf of Suez (Egyptian coast): influences of rift tectonics, climatic changes and sea-level fluctuations. In: Purser, B.H., Bosence, D.W.J. (Eds.). Sedimentation and Tectonics of Rift Basins: Red Sea–Gulf of Aden. Chapman and Hall, London, pp. 537–573.

Purser, B.H., Bosence, D.W.J. (Eds.), 1998. Sedimentation and Tectonics of Rift Basins: Red Sea–Gulf of Aden Chapman and Hall, London 663pp.

Rich, J.L., 1934. Mechanics of low-angle overthrusting as illustrated by Cumberland thrust block, Virginia, Kentucky and Tennessee. American Association of Petroleum Geologists Bulletin 18, 1584–1596.

Richard, P., 1991. Experiments on faulting in a two layer cover sequence overlying a reactive basement fault with oblique slip. Journal of Structural Geology 13, 459–470.

Rosendahl, B.R., Reynolds, D.J., Lorder, P.M., Burgess, C.F., McGill, J., Scott, D., Lambiase, J.J., Dersen, S.J., 1986. Structural expressions in rifting: Lake Tanganyika, Africa. In: Froslick, L.E., Renaut, R.W., Reid, I., Tiercelin, J.J. (Eds.), Sedimentation in the African Rifts. Geological Society of London Special Publication 25, 29–43.

Said, R. (Ed.), 1990. The Geology of Egypt Balkema, Rotterdam 734pp.

Schlische, R.W., 1992. Anatomy and evolution of the Jurassic continental rift system, Eastern North America. Tectonics 12, 1026–1042.

Schlische, R.W., 1995. Geometry and origin of fault-related folds in extensional settings. American Association of Petroleum Geologists Bulletin 79, 1661–1678.

Sharp, I.R., Gawthorpe, R.L., Underhill, J.R., Gupta, S., 2000. Fault-propagation folding in extensional settings: examples of structural style and synrift sedimentary response from the Suez rift, Sinai, Egypt. Bulletin Geological Society of America 112, 1877–1899.

Stearns, D.W., 1978. Faulting and forced folding in the Rocky Mountain foreland. Geological Society of America Memoir 151, 1–38.

Steckler, M.S., Berthelot, F., Lyberis, N., Le Pichon, X., 1988. Subsidence in the Gulf of Suez: implications for rifting and plate kinematics. Tectonophysics 153, 249–270.

Suppe, J., 1983. Geometry and kinematics of fault-bend folding. American Journal of Science 283, 684–721.

Suppe, J., 1985. Principles of Structural Geology. Prentice-Hall, New Jersey 537pp.

Trudgill, B., Cartwright, J., 1994. Relay-ramp forms and normal-fault linkages, Canyonlands National Park, Utah. Geological Society of America Bulletin 106, 1143–1157.

Twiss, R.J., Moores, E.M., 1992. Structural Geology. Freeman & Co, New York 532pp.

Withjack, M.O., Callaway, S., 2000. Active normal faulting beneath a salt layer: experimental study of deformation patterns in the cover sequence. American Association of Petroleum Geologists Bulletin 84, 627–651.

Withjack, M.O., Meisling, K., Russell, L., 1989. Forced folding and basement-detached normal faulting in the Hatenbanken area, offshore Norway. In: Tankard, A.J., Balkwill, H.R. (Eds.), Extensional Tectonics and Stratigraphy of the North Atlantic Margins. American Association of Petroleum Geologists Memoir 46, 567–575.

Withjack, M.O., Olson, J., Peterson, E., 1990. Experimental models of extensional forced folds. American Association of Petroleum Geologists Bulletin 74, 1038–1045.

Younes, A.I., Engelder, T.E., Bosworth, W., 1998. Fracture distribution in faulted basement blocks, Gulf of Suez Egypt. In: Coward, M.P., Daltaban, T.S., Johnson, H. (Eds.), Structural Geology and Reservoir Characterization. Geological Society of London Special Publication 127, 167–190.

Younes, A., McClay, K.R., 2001. Role of basement fabric on rift architecture: Gulf of Suez–Red Sea, Egypt. American Association of Petroleum Geologists Bulletin, in press.

Youssef, M.I., 1957. Upper Cretaceous rocks in Kosseir area. Bulletin de l'Institute du Desert d'Egypt 7, 35–53.